PHARMACIA

Pharmacia 70(4): 1397–1410
DOI 10.3897/pharmacia.70.e113287

Research Article

Hepatoprotective activity of QBD-based optimized N-acetyl cysteine solid lipid nanoparticles against CCL4-induced liver injury in mice

Bhavana Madupoju[1,2], Subhakar Raju Rapaka[1], Narender Malothu[1], Prasanna Kumar Desu[1], Ankarao Areti[1]

1 *KL College of Pharmacy, KoneruLakshmaiah Education Foundation, Vaddeswaram, Guntur, Andhra Pradesh 522502, India*
2 *Nalanda college of Pharmacy, Cherlapally, Nalgonda 508001, India*

Corresponding author: Subhakar Raju Rapaka (shubankarrajukluniversity@gmail.com)

Received 26 September 2023 ♦ **Accepted** 2 November 2023 ♦ **Published** 30 November 2023

Citation: Madupoju B, Rapaka SR, Malothu N, Desu PK, Areti A (2023) Hepatoprotective activity of QBD-based optimized N-acetyl cysteine solid lipid nanoparticles against CCL4-induced liver injury in mice. Pharmacia 70(4): 1397–1410. https://doi.org/10.3897/pharmacia.70.e113287

Abstract

Purpose: In the present study, *N*-acetyl cysteine (NAC)-Solid Lipid Nanoparticles (SLNs) were developed employing the Quality by Design (QBD) approach for the application of hepatoprotective activity.

Methods: Using Box-Behnken Design (BBD) three independent variables (Soya lecithin, polysorbate content, and homogenization speed) and four dependent variables (% entrapment efficiency (EE), % drug release (DR), zeta potential (ZP), and particle size (PS)) were chosen for the study. The formulations were prepared by the hot homogenization method and characterized with SEM, FTIR, DSC, and XRD and evaluated their % EE, % DR, PS, and ZP. Developed SLNs were tested for their hepatoprotective activity by an *in vivo* mice model and compared the effectiveness with free NAC and Silymarin.

Results: The optimized NAC-SLNs were found optimum with spherical and intact chemical structure (88.95% EE, 97.15% DR, -43.01 mv ZP, < 200 nm of PS) exhibiting Higuchi model of drug release. In terms of MDA levels, NAC-SLNs had a strong protective impact MDA level (23.09±0.01–21.84±0.01 u mole/mg protein) and were efficient in increasing GPx (16.89±0.01–20.71±0.02 unit/mg protein), GSH (18.94±0.57–24.21±1.00 unit/mg protein), which were reduced in the CCl_4-intoxicated group. NAC-SLNs were more effective than NAC at inhibiting the liver enzymes SGOT (150.01±1.5–132.01±0.6 mg/dL), SGPT (100.73±1.1–91.98±2.8 mg/dL), ALP (147.07±0.8–124.79±0.5 mg/dL), and LDH (290.37±3.04–228.25±2.03U/L).

Conclusion: The study concludes that NAC-SLNs therapy was not only substantially more effective than NAC, but it also had effects equivalent to a well-known hepatoprotective and antioxidant drug Silymarin.

Keywords

N-acetyl cysteine, alkaline phosphatase, Hepatoprotection, reduced glutathione, serum glutamate oxaloacetate transaminase

Introduction

Worldwide health concern research strongly states that chronic liver diseases can be the next silent epidemic which includes both alcoholic and nonalcoholic (metabolic) associated fatty hepatic diseases/disorders. The liver is a conglomerate organ that weighs about 1.5 kg in healthy humans with a diverse population of cells that differ in actions and configuration. Its composition includes parenchymal cells (80%) and non-parenchymal cells (40% possess cells like hepatic stellate, liver sinusoidal endothelial cells, and macrophages) which is 6.5% of total organ volume (Assi et al. 2021) Pr-oxidant-antioxidant state imbalance is undoubtedly stimulating and progresses a zillion chronic liver diseases like fibrogenesis, viral and alcoholic-based liver diseases which are generated by reactive oxygen species (ROS) of oxidative stress. Liver cells (kuffer, stellate, macrophages, hepatocytes, and endothelial) involved in apoptosis, ischemia, and necrotic damage reactions serve as the most efficient targeting sites for new drug carriers. Endogenous antioxidants include a set of enzymes and non-enzymes which act as scavengers of ROS. Massive molecular mass compounds (SOD, GPx, Catalase, albumin, metallothionein) and lesser molecular mass compounds (uric acid, ascorbic acid, lipoic acid, glutathione, ubiquinol, tocopherol/vitamin E, flavanone) are all examples of endogenous and exogenous free radicle scavengers (Rahal et al. 2014).

Many of the medications prescribed for the treatment of liver illnesses harm the functioning of the liver. Since there are now very few effective medication therapies for liver disease, there is a constant quest for secure, successful, as well as innovative therapy solutions. Regardless of the underlying cause, oxidative stress, or the generation of ROS, is recognized to start and control the development of hepatic disease. As a result, much research has focused on the potential therapeutic benefits of phytochemicals having major antioxidant properties (Morisco et al. 2008). The animal model of xenobiotic-induced free radicalmediated hepatotoxicity that is most well-characterized is carbon tetrachloride (CCl_4) produced liver damage. The mixed-function cytochrome P450 oxygenase system of the endoplasmic reticulum acts to produce the trichloromethyl free radical, CCl_3*, which initiates the digestion of CCl_4 by causing lipid peroxidation (LPO), a reaction that results in the generation of unstable oxygen. The last factor causes injury to the liver as well as stimulates connective tissue synthesis. Inhibiting vital cellular functions like lipid synthesis, CCl_3* attaches to cellular molecules (nucleic acid, protein, and lipid) and causes fatty acid deterioration or steatosis. It may also combine with oxygen to generate the extremely aggressive trichloromethyl peroxy radical-CCl_3OO*, that targets and annihilates polyunsaturated fatty acids linked to phospholipids. This procedure sets off a series of events of LPO (Weber et al. 2003).

A common remedy for paracetamol overdose is *N*-acetyl cysteine (NAC), which was originally used in the therapeutic environment as a mucolytic drug in the 1960s. The thiolNAC is the acetylated derivative of L-cysteine, an amino acid that functions as a building block for endogenic reduced glutathione. The replacement of depleting intracellular glutathione levels or its function as an alternate thiol substrate is hypothesized to be its mechanism of action in treating overdoses of paracetamol. NAC may also scavenge hydroxyl and peroxyl free radicals in addition to its primary function of reducing disulfide bonds and complex metal pollutants like methylmercury within the circulation (Atkuri et al. 2007). NAC is a known liver-protective antioxidant that is capable of decreasing liver damage caused by a variety of chemical groups like anesthetics (halothane, chloroform, CCl_4), industrial waste products (*N*-nitroso dimethylamine), natural products (pyrrolizidine alkaloids and amanita mushrooms), antituberculosis drugs (isoniazid, rifampicin, and pyrazinamide) and pesticide (paraquat).

Quality-based design (QBD) is used for monitoring every step involved in the process for continuous improvement of the product. Experimental designs provide maximal output (critical quality attributes) with minimum inputs (essential material properties and essential process variables). By adopting a heat homogenization method, glyceryl monostearate, soya lecithin, polysorbate 80, Tween 40, and 80 were used to create NAC-loaded SLNs in the present investigation. By applying the Box-Behnken Design (BBD) approach, the formulating process was improved.Several other metrics, including particle size (PS), Zeta potential (ZP), percent (%) entrapment efficiency (EE), drug loading (DL), XRD, Differential Scanning Colorimetry (DSC), FT-IR, and *in vivo* pharmacokinetic research tests, were assessed for the improved formulation. A well-known liver protector called silymarin (Pradhan and Girish 2006) was employed to evaluate the effectiveness of NAC-SLNs and pure NAC in light of their rapid elimination, minimal bioavailability, allergic nature, along with lack of comprehensive sub-chronic and chronic investigations assessing their liver-protective properties.

Materials and methods

Materials

The API of NAC was a gifted sample from Aravis Laboratories, Tamil Nadu. SILY API was provided by Ranbaxy Laboratories, Delhi. The solvents and reagents were obtained from SD Fine Chemicals, Mumbai. The potassium dihydrogen phosphate and disodium hydrogen phosphate were of analytical quality and were acquired from Merck India Limited, Mumbai.

Methods

Preparation of NAC-loaded SLNs

NAC-loaded SLNs were formulated using a hot homogenization method. Glyceryl monostearate (GM) and Soya

lecithin (SL) were classified in the primary analysis as solid lipids, whereas polysorbate (PS), tween 40, and tween 80 were categorized as surface active agents. NAC (50 mg) and GM (2.5 mg) along with enough lipid (soya lecithin) were weighed and merged in a water bath at 10 °C above melting point. Polysorbate with weighed amounts of hydrophilic surfactant (Tween 40 (100 mg)) and water were warmed up to the equivalent temperature in a different container while stirring frequently. The oil phase is gradually introduced into the water phase for a few hours at 1000–3000 rpm of homogenization speed. The dispersion was retained after an hour of sonication. Finally, the samples are allowed to reach room temperature and the formed SLNs were retained at 4 °C until further investigation (Madupoju et al. 2022).

Table 1. BBD experimental design elements and constraints.

Independent variables	Levels			Constraints
A:Soyalecithin content (mg)	-1	0	+1	In the range
	50	75	100	
B:Polysorbate content (mg)	50	75	100	In the range
C:Homogenization speed (RPM)	1000	2000	3000	In the range
Dependent variables				
R1: EE (%)				Maximize
R2: Drug release (%)				Maximize
R3: ZP (mV)				Maximize
R4: PS (nm)				Minimize

Characterization of optimized formulation

Effect on EE

Ultracentrifugation of the prepared NAC-SLNs was performed with a sigma 3-1KL IVD, Germany at 25,000 rpm for 30 min. UV spectrophotometric analysis of supernatant reports the free drug content. To calculate the % EE, the below calculations were employed.

$$\% \text{ EE} = (\text{Drug incorporated (mg)} / (\text{Drug in SLN (mg)} \times 100) \quad \text{eq (I)}$$

Effect of % DR

The percent drug release study of NAC-SLNs formulation was assessed through a USP-II dissolution device at 50 rpm for the initial 120 mins containing 700 mL 0.1 N HCl, then 200 mL trisodium hydrogen phosphate to preserve pH 7.4 at 37 °C. Sink conditions were maintained, and periodic sampling was performed. Sample evaluation was carried out by employing the UV-spectrophotometric technique i.e., synthesis of a chromophore product using derivatization with ninhydrin (triketohydrindene hydrate) at 493 nm in wavelength (Khushboo et al. 2015; Shrivastav et al. 2020).

Effect of PS and ZP

The Zeta sizer Nano-1000HS from Malvern Instrument Ltd., UK, was used to determine the ZP utilizing the differential light scattering (DLS) method. Milli-Q water was used to disperse nanoparticle material. At 25 °C (90 0, 50 mv), all the measurements were done in triplicate.

Scanning Electron Microscopy (SEM) study

To study the shape and structure of elements they are first encapsulated with Gold and then the particulates were subsequently placed within a SEM apparatus (FEI Quanta2 hundred MK2 from the Netherlands) to take the visualizations of SLNs (Ram et al. 2015).

In vitro drug release study

In order to estimate the release of NAC from SLNs, the dialysis bag method was employed.

A dialysis bag with a molecular weight cutoff of 12,000–14,000 Da was used to hold 0.5 g of nanoparticulate dispersions (equivalent to 40 mg of NAC) was added to 1000 ml of dissolution media. The pH 7.4 phosphate buffer, which was agitated at 100 rpm at 37 0.2 °C, was poured into an open-ended bag. 0.5 ml of the removed sample was replaced with fresh dissolving medium. A Ninhydrin based UV spectrophotometer technique was used to determine the concentration of NAC in the sample after the proper dilution. Data on in vitro drug release was fitted to various kinetic models to ascertain the medication's mechanism of action (El-Housiny et al. 2018).

FT-IR study

Compatibility testing of the pure drug and the optimized formulation was carried out by FTIR spectrophotometer (Perkin Elmer Spectrum One, Waltham, Massachusetts, USA) from a range of 4000 to 400 cm^{-1}.

DSC study

DSC (DSC Q10 V9.0 Build 275) was used to analyze the degree of compatibility of excipients and drugs with the medication. A heating rate of 0 to 1000 °C at 15 °C per min in a hermetically sealed cabin was used to construct the thermographs.

XRD study

Crystalline nature of the sample can be analyzed using X-ray Diffractometer (Bruker, Germany). Cu Ka radiation with a wavelength of 1.5406 with a voltage of 40 kV and a current of 40 mA (angle range of 3–40° across a distance of 2 with a count time of 0.3 seconds and a step angle of 0.02°) were the specifications used for improved NAC-SLNP formulation (Rahman et al. 2023).

Animal studies

Male Swiss albino mice (30–35 g) were purchased and acclimated to laboratory settings by placing them into polypropylene housings in a room with a thermostat for a week before the experiment began. The animals were given regular pellet food and unlimited access to water. The Institutional Animal Ethics Committee (IAEC) approved, and CPCSEA procedures were adhered to throughout the investigation at Nalanda College of Pharmacy, Nalgonda (CPCSEA REGD.NO. 318/Re/s/2001/CPCSEA, IAEC Approval NO: NCOP/IAEC/00075).

Experimental design

The Swiss albino male mice were divided into nine groups of six animals each and an oral route of administration was employed for the experimental study.

For the first two weeks, Group I animals were given 1 ml/kg BW olive oil twice a week, followed by 1.5 ml/kg for the next two weeks; Group II animals were given 1 ml/kg BW CCl_4 (combined with an equivalent amount of olive oil) 2 times a week for the initial two weeks, followed by 1.5 ml/kg BW for the next two weeks; Group III was treated with 1.75 mg/kg BW – low dose [LD] of NAC-SLNs and CCl_4; Group IV treated with 2.5 mg/kg BW – medium dose [MD] NAC-SLNs and CCl_4; Group V treated with 3.25 mg/kg BW – high dose [HD] NAC-SLNs and CCl_4; Group VI treated with 1.75 mg/kg BW –low dose [LD] NAC and CCl_4; Group VII treated with 2.5 mg/kg BW – medium dose [MD] NAC and CCl_4;Group VIII treated with 3.25 mg/kg BW – high dose [HD]) NAC and CCl_4 and Group IX received normal treatment (SILY). SILY was administered at a dose of 25 mg/kg BW per day for four weeks (distributed in 0.7% w/v carboxy methyl cellulose in water). Animals were sacrificed at the end of the treatment and serum was collected. Centrifugation at 2500 rpm for 15 mins was employed to separate serum and perform testing for antioxidants and biochemical evaluations.

Biochemical parameters

Estimation of lipid peroxidation (LPO)

The measurement of malondialdehyde was used to calculate LPO. The reaction solution contained 0.2 mL of tissue extract, 10% TBA, 2 mM sodium pyrophosphate, and 0.3 M Tris HCl buffer (pH 7.4). This was incubated for 30 mins at 37 °C with continuous shaking. To stop the reaction, 1 mL of 10% TCA was applied after incubation. After 20 mins in a boiling water bath, the mixture was subjected to 5 mins of centrifugation at 2000 rpm. Standard tubes of 10, 20, 30, 40, and 50 nmol/mL were used at the same time. The hue created in the tubes was measured at 532 nm after centrifugation. The sample's MDA content is measured in nanomoles of MDA per milligrams protein (Rampaka et al. 2021).

Antioxidant assays Enzymatic antioxidant-Glutathione peroxidase (GPx)

The activity of GPx was measured using the method described by Rotruck et al. (1973) technique The interaction of reduced glutathione with the 5,5´-dithiobis-(2-nitrobenzoic acid (DTNB) solution. The blend consisted of 0.4 M sodium phosphate buffer (pH.7), 10 mM sodium azide, 4 mM reduced glutathione, 2.5 mM H_2O_2, and 0.1 ml tissue extract. The volume was increased to 2.0 ml with deionized water and incubated for 10 mins at 37 °C before being halted by the inclusion of 10% TCA. The mixture underwent centrifugation for 3 mins at 3000 rpm. DTNB and 0.3 M disodium hydrogen phosphate were added to the supernatant. Using a spectrophotometer, the yellow color generated was measured at 412 nm against a reagent blank containing phosphate buffer solution and DTNB reagent. Standard aliquots were likewise processed similarly. The enzyme activity was measured in units per milligram of protein (1U is the amount of enzyme that converts 1 mol reduced glutathione (GSH) to GSSG per minute in the presence of hydrogen peroxide) (Ohkawa et al. 1979).

Non-enzymatic antioxidant Reduced glutathione (GSH)

GSH was determined by the method of Moron et al. (1979) The GSH content was estimated by suspending 0.1 mL of tissue homogenate with an equal volume of TCA (10%). The contents were centrifuged to remove the precipitate. From this, the supernatant was taken and made up to 2.0 mL with phosphate buffer (pH 8; 0.2 M). It was followed by the addition of 0.5 mL Ellman's reagent (DTNB reagent). After 10 mins, the absorbance was measured spectrophotometrically at 412 nm in contrast to a blank containing 2.0 mL Phosphate buffered saline (PBS) and 0.5 mL DTNB. The values were displayed as units (nanomoles) per milligram of protein (Rotruck et al. 1973).

Liver toxicity markers

Assay of serum glutamate oxaloacetate transaminase (SGOT)

Reitman and Frankel's (1957) technique was used to estimate the SGOT levels. By converting oxaloacetate to pyruvate using aniline citrate, the quantity of oxaloacetate was determined. 2, 4 – dinitro phenyl hydrazine (2,4-DNPH) was used to react with the produced pyruvate. The spectrophotometric reading of the brown color generated was taken at 520 nm. 1 mL substrate was pipetted into two test tubes and put in a 37 °C water bath for a few mins. 0.2 mL of serum was added to one of the test tubes and gently shaken. Two drops of aniline citrate reagent were applied to both tubes and left for 20 mins while the tubes were still in the water bath. Then 1 cc 2,4-DNPH was added to each tube and left for another 20 mins. After incubation, the tubes were removed from the water bath and 10 mL of 0.4 N sodium hydroxide was added. After 10 mins, the tubes were read at 520 nm. The results were represented in micrograms per milliliter of serum (Alam et al. 2013).

Assay of Serum Glutamate Pyruvate Transaminase (SGPT)

SGPT was assayed by the method of Reitman and Frankel (1957) The amount of pyruvate formed was measured by treating it with 2,4-DNPH. The brown color developed was read in a spectrophotometer at 520 nm. In two tubes, 1 mL of the substrate was added and put in a 37 °C water bath. According to one tube, 0.2 mL serum was added and gently shaken to combine 2 drops of aniline, exactly half an hour later both test tubes were filled with citrate reagent and stored in a water bath. For 20 mins, these two

tubes were left alone. 1 mL of 2,4DNPH was added, and the mixture was allowed to sit for another 20 mins. The tubes were then taken out of the water bath and 10 mL 0.4 N sodium hydroxide was added. After 10 mins, the OD was measured at 520 nm. The results were given in the form of IU/mL of serum (King et al. 1934).

Estimation of Alkaline Phosphatase (ALP)

Phosphatases are enzymes that catalyze the phosphoric acid separation from monophosphoric esters. At pH 10.0, alkaline phosphatase liberates inorganic phosphorus from sodium glycerophosphate. This phosphorus was allowed to react with molybdic acid to form phosphomolybdate, which was then reduced to molybdenum blue by ANSA (1-amino, 2- naphthol, 4-sulphonic acid). 1 mL buffered substrate (0.1 M sodium glycerophosphate dissolved in sodium carbonate) tissue extract was added to 0.2 mL of bicarbonate buffer (0.1M, pH 10.0) and incubated at 37 °C for one hour. Following the incubation period, 10% TCA was added, mixed, and centrifuged for 10 mins. Ammonium molybdate and ANSA were added to an equal amount of supernatant. A spectrophotometer set to 680 nm was used to read the color generated. As a control, an enzyme-free system was used. A set of standards with concentrations ranging from 0.156 to 0.781 moles were likewise treated in the same way. The enzyme activity was measured in micrograms per liter of serum (Ringoira and Plumb 1975).

Estimation of Lactate dehydrogenase (LDH)

The quantity of LDH was calculated using the Ringoir and Plum technique (1975) The tubes were left to incubate at 37 °C for 10 mins after adding 1 mL of the substrate (Lithium lactate – 21.9 mL of glycine, 13.1 mL of 0.1 NaOH, and 0.7 g of lithium lactate) to 0.1 mL of sample. This was mixed thoroughly, and then 0.2 mL NAD was included. It was then incubated at 37 °C for 15 mins. Following that, 0.4 N NaOH was added. At 450 nm, the absorbance was measured (Ye et al. 2009).

Histopathological examination

Liver tissue was obtained, fixed in 10% formalin, and paraffin slices of 5 µm thickness were produced and stained with hematoxylin and eosin. Under a microscope, the pathological alterations were investigated (del Rio et al. 2005).

Statistics

Every outcome was presented as mean ± SD. Individual comparisons were obtained using LSD and one-way ANOVA. Significant differences between groups were determined using one-way analysis of variance and the T-test in GraphPad Prism 8.0. Asterisks (*) are used to indicate statistical differences from the healthy group (Group I) and CCl_4-induced group (Group II) when the $p < 0.05$.

Results

Preparation of NAC -loaded SLN formulations

A total number of fifteen NAC-loaded SLNs were prepared as per ratios suggested by the Box -Behnken experimental model of Design Expert software. They were subjected to evaluation parameters like EE, DR, ZP, and PS and the results were mentioned in Table 2.

Statistical analysis and optimization of NAC-SLNs by BBD

In the present study, a 15 run of BBD was preferred to optimize the NAC-loaded SLN by minimizing the PS and maximizing the % EE and % DR. The autonomous variables preferred in the present study were the Soya lecithin content (A), Polysorbate content (B), and homogenization speed (C). R1: EE (%), R2: DR (%), R3: ZP (mV), and R4:PS (nm) were selected as dependent variables. To ascertain the impact of independent factors on

Table 2. Experimental lattice and acquired outcomes from randomized runs in BBD.

Formulation Code	A: Soya lecithin content(mg)	B: Polysorbate content (mg)	C: Homogenization speed (rpm)	R1: EE (%)	R2: DR (%)	R3: ZP (mV)	R4: PS (nm)
NAC-SLN 1	100	75	1000	71.25	89.35	-32.03	157.37
NAC-SLN 2	50	75	3000	63.59	81.56	-39.13	98.28
NAC-SLN 3	100	50	2000	82.35	91.31	-38.36	152.41
NAC-SLN 4	50	50	2000	75.25	83.28	-49.47	89.02
NAC-SLN 5	75	75	2000	73.18	89.76	-51.32	138.56
NAC-SLN 6	75	75	2000	78.95	91.75	-39.32	142.16
NAC-SLN 7	75	50	3000	68.93	80.91	-40.12	100.69
NAC-SLN 8	75	75	2000	72.56	84.28	-40.2	145.4
NAC-SLN 9	100	75	3000	80.69	93.24	-43.32	158.02
NAC-SLN 10	50	75	1000	89.32	96.25	-50.33	128.37
NAC-SLN 11	75	50	1000	84.36	90.86	-49.28	142.9
NAC-SLN 12	75	100	3000	80.21	92.77	-42.16	142.54
NAC-SLN 13	75	100	1000	82.35	92.56	-39.47	147.34
NAC-SLN 14	100	100	2000	78.25	93.28	-38.32	169.85
NAC-SLN 15	50	100	2000	83.18	91.31	-37.32	125.56

the dependent variables, regression analysis was carried out. The summary of the regression analysis was given in Table 3. A 2FI model equation was produced by the regression analysis. for all the dependent variables. The importance of three factors chosen during the preliminary research determined the applicability of the PS model, such as the Soya lecithin content (A), Polysorbate content (B), and Homogenization speed (C). The outcomes of an ANOVA for specific responses (EE (R1), DR (R2), ZP (R3), and PS (R4)) were given in Table 3. 3-D response surface graphs for chosen responses EE, DR, ZP, and PS were given in Fig. 1.

Table 3. ANOVA studies of the BBD-designed NAC-SLNs.

Response	Model	R^2	Adjusted R^2	Predicted R^2	Adeq precision	F value	P value
EE	2FI	0.8662	0.7659	0.5958	11.6556	8.63	0.0038
DR	2FI	0.8727	0.7772	0.7578	9.5030	9.14	0.0032
ZP	2FI	0.7360	0.5380	0.5097	6.6200	3.72	0.0455
PS	2FI	0.9658	0.9402	0.8915	18.8645	37.67	0.0001

The results of the prepared formulations were fitted into various polynomial model equations which revealed that the independent variables (EE, DR, ZP, and PS) have a 2FI interaction effect on the observed responses. From the above Table 3, it is visible that the independent variables have enhanced multiple correlations, adjusted as well as the predicted, sum of squares and significant statistical terms at the selected probability level. Statistics for all responses proven that there is a reasonable agreement between the predicted R^2 and adjusted R^2 values (the difference is <2). In the present study, an adequate precision ratio greater than 4 is desirable it measures the signal-to-noise ratio that aids in navigating the design space. Validation of the obtained polynomial equations was done by ANOVA and found to be statistically significant ($p<0.05$). Numerical and graphical optimization results with 2D and 3D-surface response plots further aid to investigate the interactive effects of critical product parameters (CPP) on critical quality attributes (CQA). This surface methodology plot helps to interrogate the effect of two CPPs simultaneously by keeping others at a constant level at every response. Using perturbation and interaction plots we can quantify and compare two parameters at each point by stabilizing the other. The desirability function for PS was chosen as a minimum, for ZP it is in range, and for % DR & % EE is the maximum level.

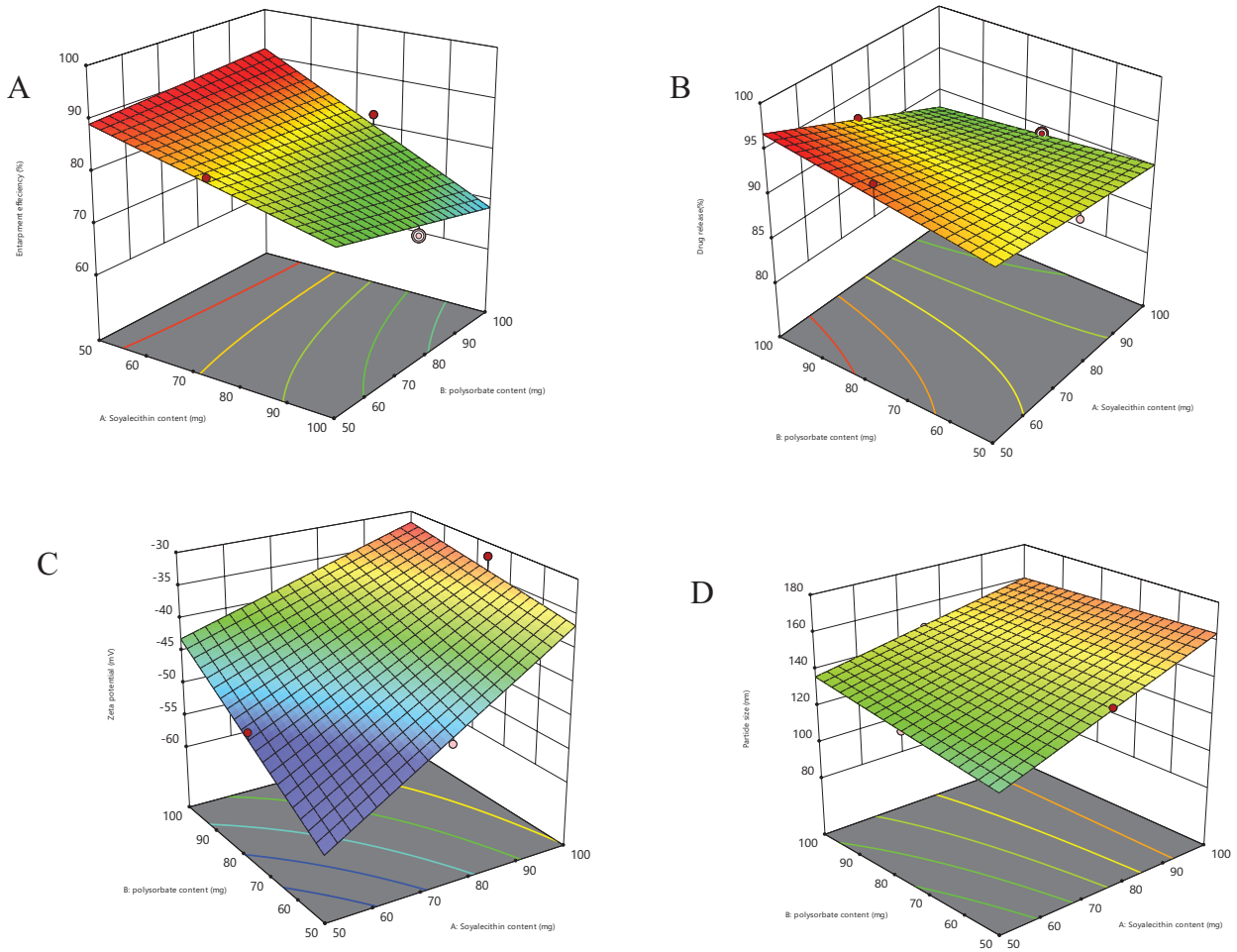

Figure 1. A–D 3D-response plots represent the impact of CMAs on (GMS content, Polysorbate content, and homogenization speed) on (**A**) % EE (**B**) % DL (**C**) ZP (mV) and (**D**) PS (nm).

Effects on EE

The polynomial expression that the investigation produced is given by:

$$EE=+77.63+0.1500*A+1.64*B-4.23*C-3.01*AB+8.79*AC+3.32*BC \quad eq(II)$$

The quantitative expression of A, B, and C on responses are expressed in the above equation. The magnitude of the coefficient describes the effect of the variable on the response, which shows all the values of coefficients on each response. Even the statistical analysis strengthens the above equation i.e., F>P<0.05. The positive sign and value of the coefficient explain how the independent variable acts on the response, the "+" acts as a synergistic, and "- "acts as an antagonistic act on the response. In this context out of all the independent variables A (Soya lecithin content), B (Polysorbate content), and AC (interactive coefficient) show significant impact whereas C (homogenization speed), AB, BC (Interactive coefficients) show a little impact on the responses (EE, DR, ZP, PS). Increased GMS and Polysorbate content increase the drug accommodation and increased homogenization speed leads to reduction. Fig. 1 shows the 3D plots showing the impact of independent variables on the responses. The obtained range of EE from the results is 63±1.20 (NAC-SLN2) to 89.32±2.41 (NACSLN10).

Effects on DR

The polynomial expression that the investigation produced is given by:

$$DR =+89.50+1.85*A+2.95*B-2.57*C-1.15*AB+4.65*AC+2.54*BC \quad eq\ (III)$$

Statistical analysis strengthens the above equation (F>P<0.05). Among all the independent variables A (Soya lecithin content), B (Polysorbate content), C (homogenization speed), and AC (interactive coefficient) show a remarkable impact, whereas AB, AC (Interactive coefficients) shows little impact on the responses (EE, DR, ZP, PS). Increased Soya lecithin and Polysorbate concentrations increase the drug release and increased homogenization speed leads to its reduction. Fig. 1 shows 3D plots showing the impact of independent variables on the responses. The obtained range of DR from the results is 81.56±3.36 (NAC-SLN2) to 96.25±4.11(NAC-SLN10).

Effects on ZP

The polynomial expression that the investigation produced is given by:

$$ZP = -42.01+3.03*A+2.50*B+0.79*C-3.03*AB-5.62*AC-2.96*BC \quad eq(IV)$$

Statistical analysis strengthens the significance of the Values of coefficients in the above equation (F>P<0.05). Among all the independent variables AC (interactive coefficient) shows a significant effect whereas other coefficients show a little impact on the responses (EE, DR, ZP, PS). Increased soya lecithin and Polysorbate concentrations increase the Zeta potential and increased homogenization speed leads to its reduction. Fig. 1 shows 3D plots showing the impact of independent variables on the responses. The obtained range of DR from the results is -32.03±1.27 (NAC-SLN1) to -50.33±2.05(NAC-SLN10).

Effects on PS

The polynomial expression that the investigation produced is given by:

$$PS=+135.90+24.55*A+12.53*B-9.56*C-4.78*AB+7.68*AC+10.27*BC-13.54*AB+20.63*AC+10.27*BC-13.54*A2-28.74*B2-6.57*C2 \quad eq(V)$$

Independent variables A, B, and C show significant effects whereas other coefficients act as a significant role in the responses (EE, DR, ZP, and PS). Increased soya lecithin and polysorbate concentrations show a progressive impact on the size of the nanoparticles. Fig. 1 shows 3D plots showing the impact of independent variables on the responses. The obtained range of PS from the results is -89.02±3.32 (NAC-SLN4) to 169.85±4.64 (NACSLN10). Statistical data strengthens the significance of the values of coefficients in the above equation (F>P<0.05).

Optimization and validation of the model

All 15 formulations designed using BBD design were subjected to an experimental trial. The desirability function was utilized to optimize the independent variables for all responses. Based on the desirability value (0.778) all four responses (R1: EE, R2: DR, R3: ZP, R4: PS) were transfigured into desirability scales as mentioned in Fig. 2, NAC-SLN10 formulation was selected as the optimized formulation. an overlay plot shows two regions yellow indicates the possible criteria for obtaining optimized formulation and grey indicates no possibility. The optimum formulation depicted as per the overlay plot shows the following desirability criteria: EE (%): 90.52, DR (%): 94.89, ZP (mV):-51.32, PS (nm): 128.71. Independent variables desirability specifications include soya lecithin Content: 50 mg, Polysorbate content: 75 mg, and Homogenization speed:1000 RPM.

Effect on EE

The EE (%) of all formulations was given in the Table 2 the range lies from 63±1.20 (NACSLN2) to 89.32±2.41 (NACSLN10). The % EE of the prepared optimized formulation was found to be 88.95%.

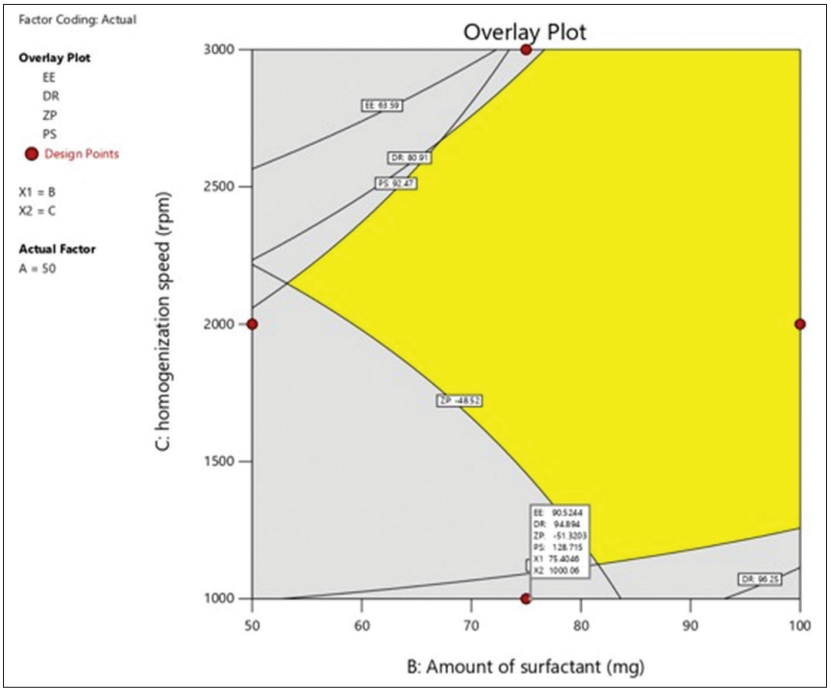

Figure 2. Desirability and overlay plot of optimized formulation (NAC-SLN 10).

Table 4. Characterization of optimized formulation (NAC-SLN 10).

Characterization	Predicted	Observed
EE (%)	90.52	88.95
PZ (nm)	128.71	100.1
ZP (mV)	-51.32	-43.1
In vitro drug release (%)	94.89	97.15

Effect on % DR

The % drug release of all the 15 formulations was mentioned in Table 2 and the % DR of the prepared NAC-SLN10 was found to be 97.15% for 8 hrs.

Effect on PS and ZP

The mean PS (Fig. 3) of optimized NAC-SLNs was found to be between 96.02 nm to 110 nm (NAC-SLN10).

The ZP or change in the surface of colloidal particles in *N*AC-SLN was studied to determine the charge on the particles to avoid agglomeration. Fig. 4 indicates the ZP of the optimized formulation as -38.01 mV (NAC-SLN10).

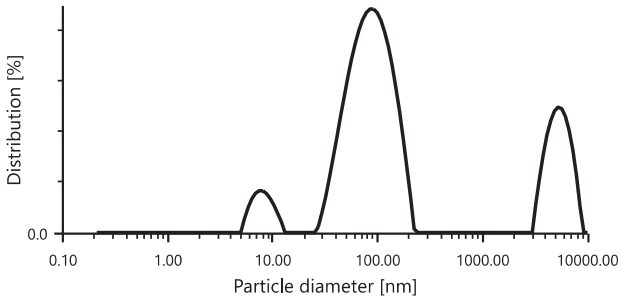

Figure 3. PS distribution graph of pure drug and optimized formulation (NAC-SLN10).

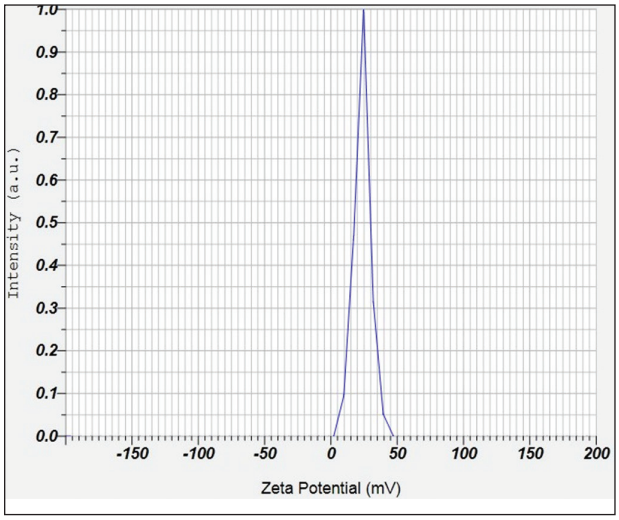

Figure 4. ZP graph of optimized formulation (NAC-SLN10).

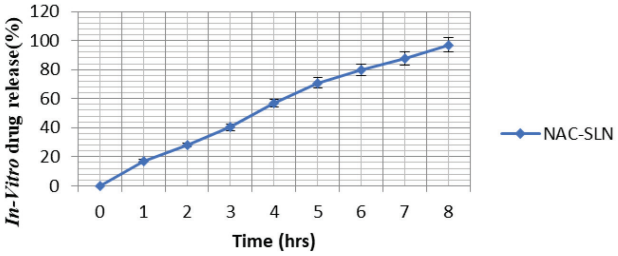

Figure 5. *In vitro* drug release profile of optimized formulation (NAC-SLN10).

In vitro drug release

The cumulative drug release of optimized formulation (NAC-SLN10) was found to be 97.15% for 8 hrs. With almost 95% of the entire drug quantity released within

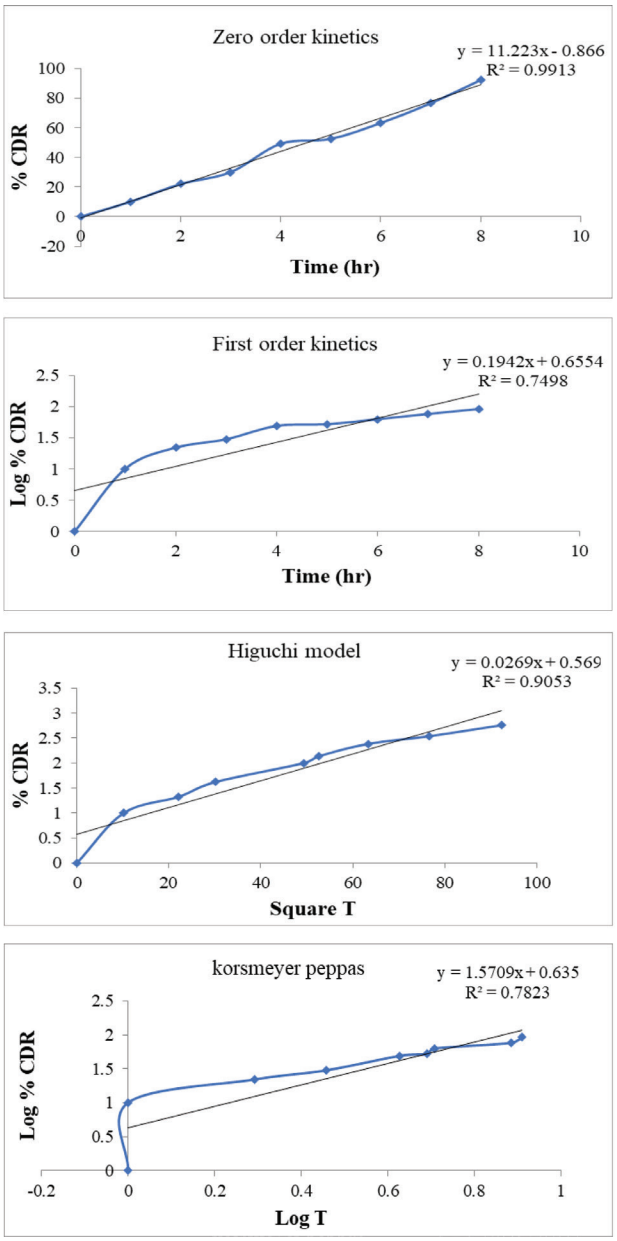

Figure 6. Drug release kinetics of the optimized formulation (NAC-SLN10).

8 hours, SLN exhibited a steady release pattern. Due to the drug's decreased mobility in the solidified form of the binary lipids, SLN demonstrated the shortest release rate. The Higuchi matrix model provided the best fit for the release kinetics of the system.

SEM

SEM images of the optimized NAC-SLNs were found to be spherical with smooth surface finishes with a particle diameter of <130 nm.

FT-IR study

The amide (bending, NH) peak was observed at 3758.46 cm^{-1}, while the SH and C=O carboxylic stretching peaks appeared at 2979.50 cm^{-1} and 1520 cm^{-1}, respectively. Both the carboxyl group and the amide group were likely involved in the design of different hydrogen bonds in the multi-composite compound because the peaks at 2976.41 cm^{-1} and 3736.41 cm^{-1} are shifted concerning the spectrum of pure active ingredient NAC, respectively. The graphs show that the characteristic peaks of NAC were still discernible and that the band lengths in the optimized formulation stayed unchanged, indicating that NAC was compatible with the other chemicals in the formulation and did not degrade.

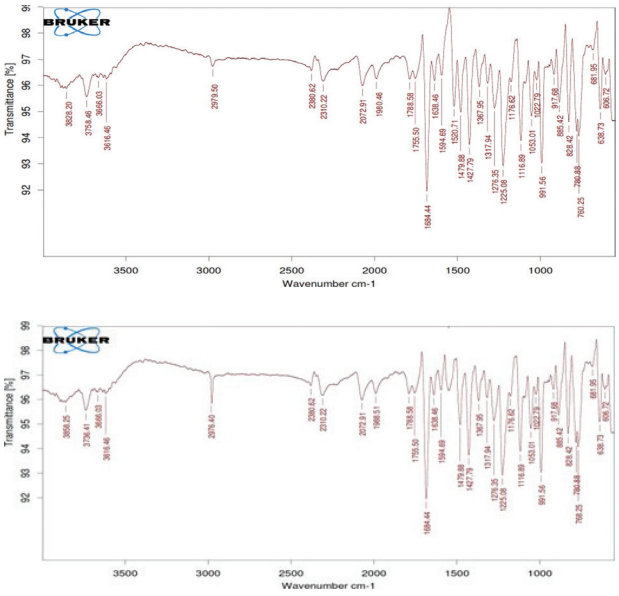

Figure 7. FTIR graphs of pure drug and optimized formulation (NAC-SLN10).

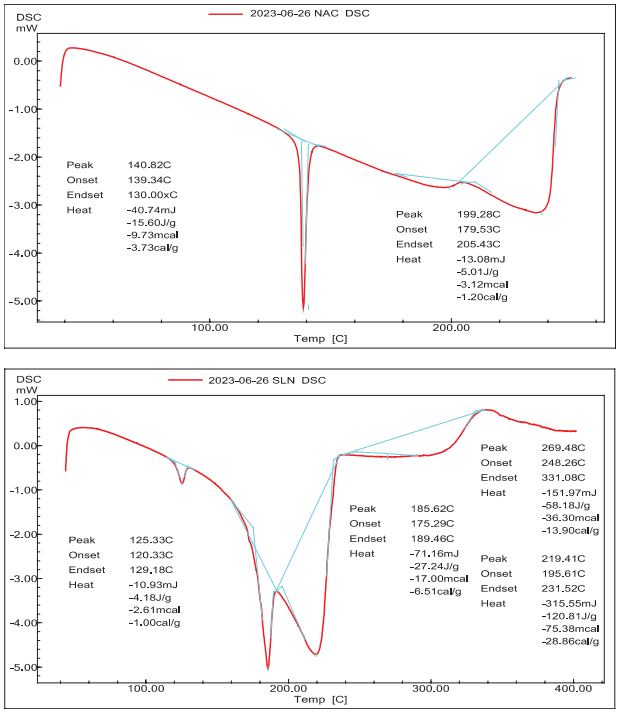

Figure 8. DSC analysis of pure drug (NAC) and optimized formulation (NAC-SLN 10).

DSC study

The thermographs indicate homogeneous dispersion of NAC in the optimized formulation as the endothermic peak (MP of NAC ΔH=-15.60J·g $^{-1}$) is intact in the formulation thermograph.

XRD study

Fig. 9 illustrates the X-ray diffraction spectra of pure NAC and NAC-SLNs. NAC disclosed clearly identifiable, intense peaks between 12° and 28°, but when the SLNs were loaded with the drug, the intensity of the peaks reduced, pointing to the medication's amorphous state as a result of its entrapment.

Effect of NAC-SLNs on antioxidant levels

The effects of treatment were similar in the case of the enzymatic and nonenzymatic antioxidants. The NAC-derived SLNs were effective in promoting the enzymatic and nonenzymatic antioxidants which were decreased in CCl_4 intoxicated group (Fig. 11).

Effect of NAC-SLNs on liver enzymes and LDH

The levels of SGOT, SGPT, and ALP were taken as indicators of liver injury. In CCl_4 intoxicated group, these enzyme levels were inclined to higher levels (Fig. 13). These levels were invigorated to normal levels by treatment with

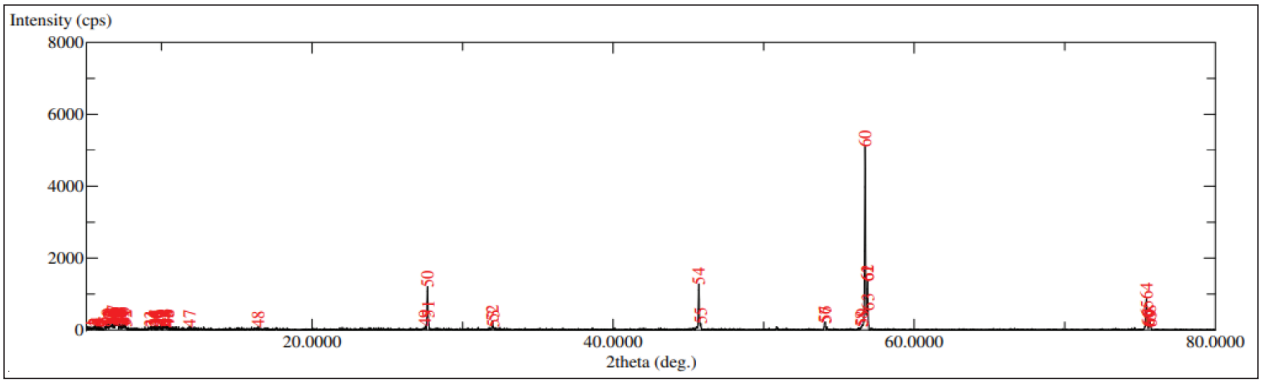

Figure 9. XRD studies of the optimized NAC-SLN formulation.

Effect of NAC-SLNs on LPO

The level of LPO was directly proportional to its end product MDA. MDA levels were increased in CCl_4 intoxicated group. These levels were brought back to near-normal levels by treating with SLNs synthesized using NAC. The NAC also possessed a significant protective effect considering the levels of MDA. In comparison with SILY (25 mg/kg BW) effectively combated MDA levels (Fig. 10).

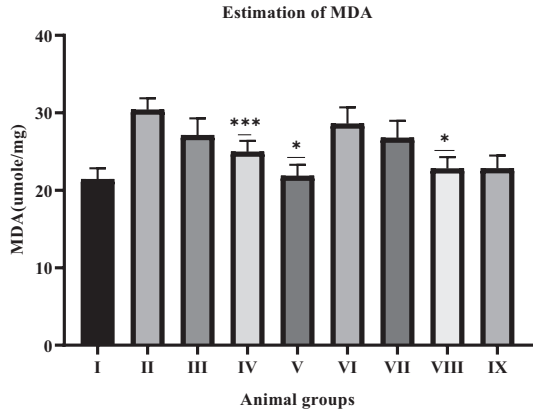

Figure 10. Effect of SLNs loaded with NAC and NAC on lipid peroxidation.

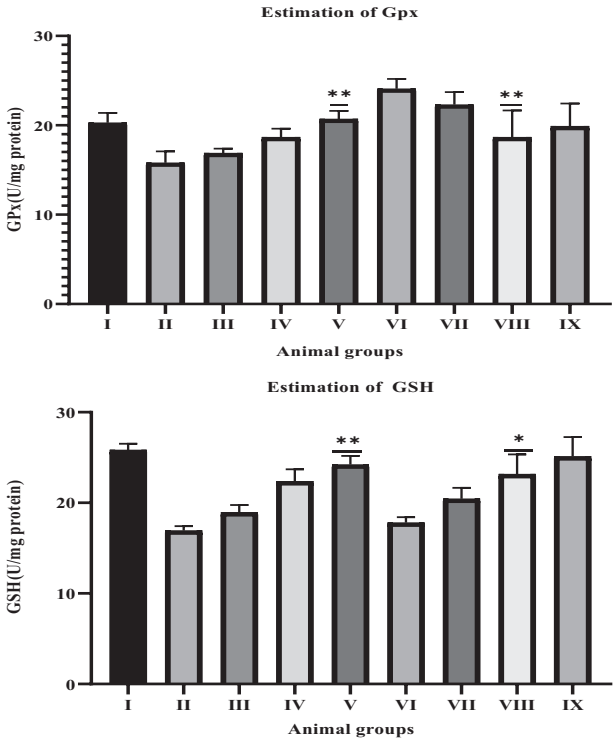

Figure 11. Effect of SLNs loaded with NAC and NAC on GPx and GSH.

NAC-SLNs. The cellular metabolite LDH was increased in the CCl_4 intoxicated group, which was brought back to normal levels by treatment with SLNs (Fig. 12). Regarding the liver enzymes and cellular metabolite LDH, NAC SLNs were effective in the treatment in comparison to NAC.

Effect of NAC loaded SLNs on hepatic architecture

Hepatic architecture was altered, and improperly organized hepatic cells were visible in the CCl_4-impaired group. Hepatic cells in the liver sections of healthy animals had distinct cytoplasm, pronounced nuclei, and well-prominent central veins. The animal in the control group displayed complete destruction of the hepatic architecture, including centrilobular hepatic necrosis, vacuolization, and a fragmented central vein. In treatment groups, these consequences were revived with their original architecture (Fig. 14).

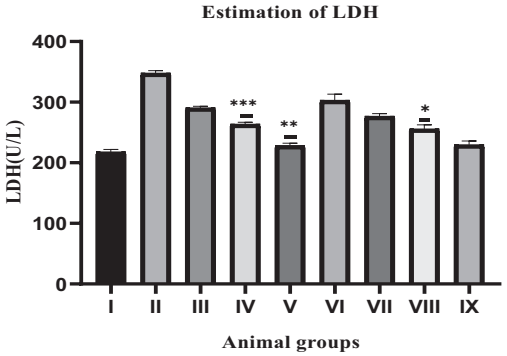

Figure 12. Effect of SLNs loaded with NAC and NAC on LDH.

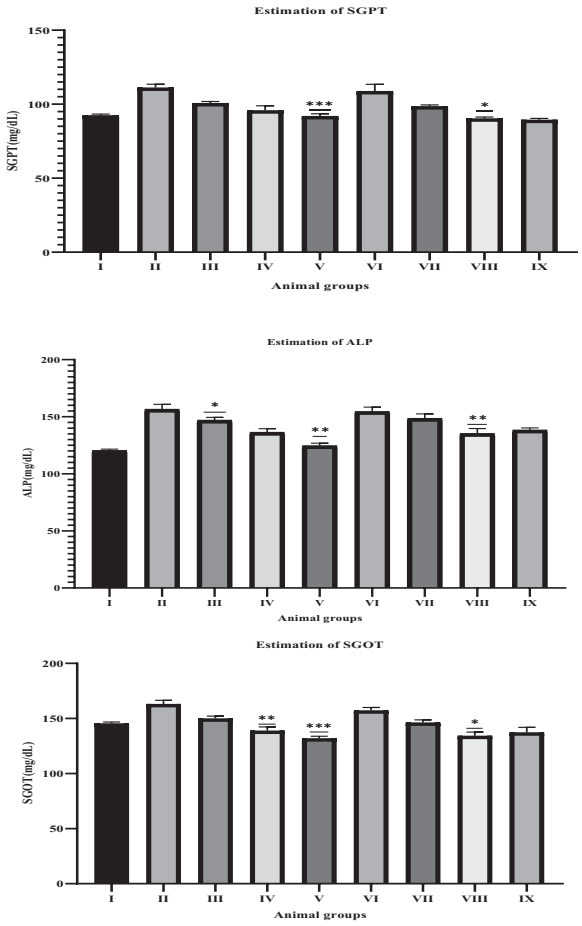

Figure 13. Effect of SLNs loaded with NAC and NAC on SGPT, SGOT, and ALP.

Discussion

LPO is an autocatalytic process, which is a general outcome of cell death. This process may result in peroxidative tissue damage as a result of the toxicity of xenobiotics. MDA is one of the end products of LPO, which is commonly accepted as an indicator of LPO and thereby oxidative stress (Reitman and Frankel 1957). When it comes in contact with DNA and proteins, they tend to be mutagenic and atherogenic. Due to the toxicity caused by CCl_4, MDA levels were elevated as a result of peroxidative damage to the liver, which was reestablished back to normal by treated therapy.The equilibrium of ROS is maintained by the amount they produce under normal circumstances and eventual elimination by enzymatic (GPx) or non-enzymatic antioxidants (GSH). It has been demonstrated that enzyme-based antioxidants may effectively combat oxidative stress. One of the renowned indicators for hepatotoxicity is GPx, which converts H_2O_2 to non-toxic products such as water. GPx was decreased in the injury-induced group.

The control group had inadequate amounts of GSH, the first line of defense against oxidative stress. This decrease might be due to the reduction of NADPH or utilizing GSH to exclude peroxides (Hsu et al. 2010). These effects were revived efficiently by the administration of SLNs, identical to the findings from the standard group that received conventional medication therapy. The control group exhibited higher liver enzyme values than the normal group, including SGOT, SGPT, and ALP. The hepatocyte damage in the CCl4-treated group is shown by the elevated blood enzyme levels (Upur et al.2009). Higher quantities of liver enzymes in the blood are indicators of a damaged liver. This results from integrity in cell loss and serum enzyme leakage brought on by lipid peroxidation. Parallel to the standard treatment group, the SLNs-treated groups' liver enzymes returned to levels close to normal.

LDH facilitates the conversion of pyruvate and lactate into energy and catalyzes these processes instantly using NADH and NAD+, which acts as a marker for hepatocellular necrosis. LDH, an enzyme that breaks down glucose and is used as an indicator for tissue damage, had elevated levels in the control group but improved in the treatment groups (Thapa and Walia 2007). SLNs were more prevalent in restoration comparison to the plant extract in both

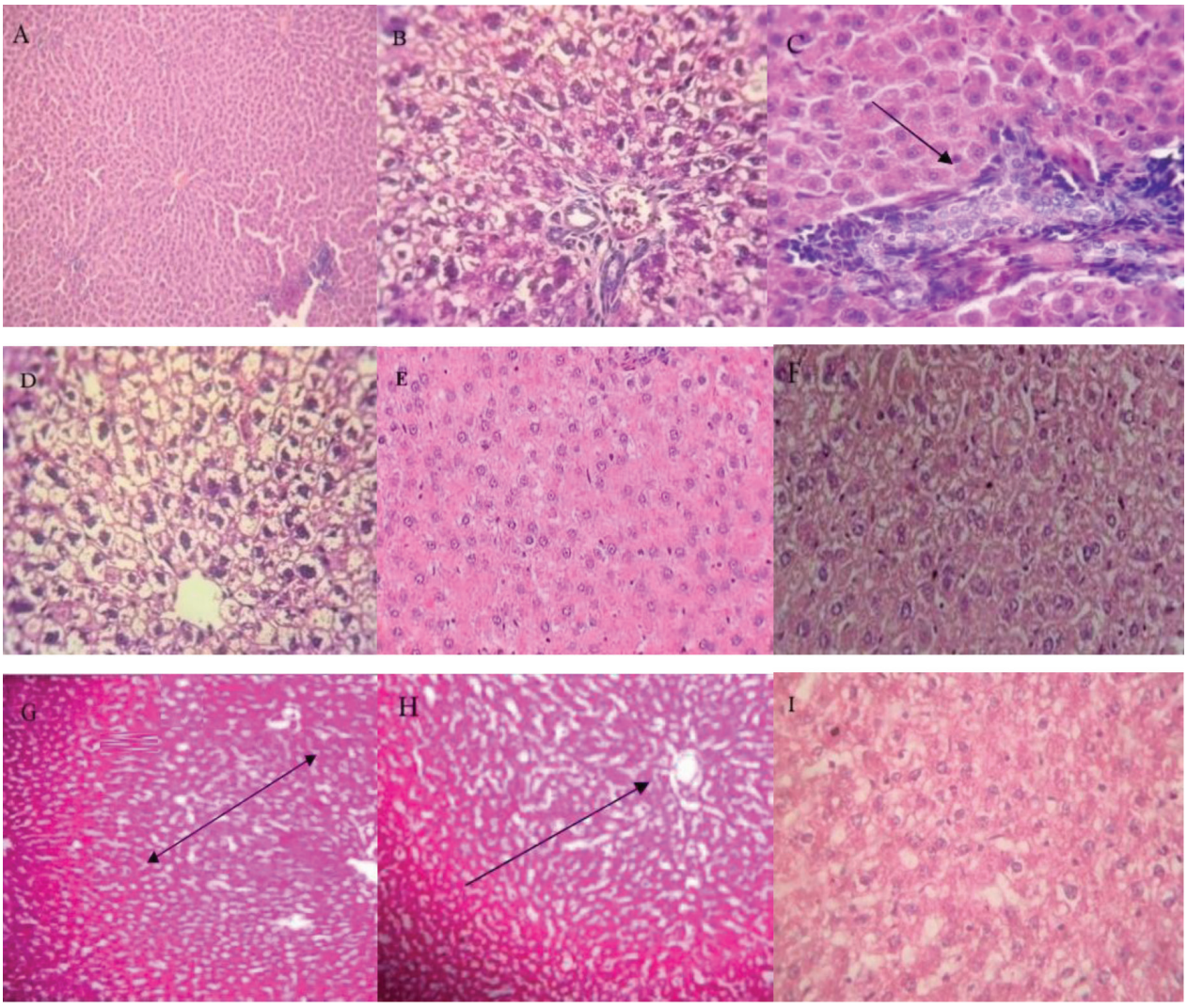

Figure 14. Histopathological profile **A.** Intact, **B.** Control, **C.** CCl_4 + LD NAC-SLN, **D.** CCl_4 + MD NAC-SLN, **E.** CCl_4 + HD NAC-SLN, **F.** CCl_4 + LD NAC, **G.** CCl_4 + MD NAC, **H.** CCl_4 +HD NAC, **I.** CCl_4 + SILY.

Table 5. Biochemical parameters as a comparison between NAC and NAC-derived SLNs.

Groups	LDH (U/L)	MDA(µmole/ mg protein)	GPx (unit/mg protein)	GSH (U/mg protein)	SGOT (mg/dL)	SGPT (mg/dL)	ALP(mg/dL)
Group I	217.73±1.27	21.41±0.03***	20.29±0.03	25.82±0.54***	152.20±1.0	92.54±0.9**	120.61±0.6
Group II	347.74±2.88	30.38±0.02	15.80±0.03**	16.93±0.36	163.15±0.6	111.25±0.4	156.70±0.8**
Group III	290.37±3.04	23.09±0.01	16.89±0.01	18.94±0.57**	150.01±1.5	100.73±1.1	147.07±0.8
Group IV	263.37±2.10***	24.96±0.53***	18.67±0.02	22.36±0.13	138.93±0.6	95.88±0.7	136.45±0.9
Group V	228.25±2.03*	21.84±0.01*	20.71±0.02**	24.21±1.00***	132.01±0.6**	91.98±2.8**	124.79±0.5**
Group VI	303.03±3.08**	28.59±0.01	24.09±0.01	17.80±0.55	157.28±0.9	108.87±0.6***	154.70±0.6
Group VII	276.56±1.01	26.76±0.02	22.30±0.01	20.44±0.04	146.29±0.7	98.65±0.8	148.63±1.1
Group VIII	255.56±1.01*	22.76±0.02*	18.66±0.02*	23.16±0.08*	134.29±1.6*	90.39±0.5	135.45±1.4*
Group IX	229.26±1.01	22.81±0.05	19.89±0.02	25.12±0.01	137.36±0.6	89.49±0.3	138.45±0.7

Results were expressed as mean ± SD ($p<0.05$).*=$P<0.05$,**=$P<0.01$,***=$P<0.001$.

cases, bringing the elevated enzyme level in the injury-induced group back to close to normal. The histopathological analysis provided supportive evidence for the hepatoprotective efficacy of SLNs.

The therapeutic impact of the studied nanoparticles was dose dependent. The LD and MD SLNswere limited in effect in treatment in the case of NAC-derived SLNs compared to HD SLNs. The dose might not be enough to induce considerable physiological effects compared to the HD-treated group (Kim et al. 2010). The antioxidant potential has been associated with components' protective impact against liver damage. Oxidative stress and liver damage are generated when the antioxidant system's capacity to scavenge free radical's declines. Positive therapeutic effects on liver damage brought on by CCl_4 can be attained by bolstering the antioxidant defense system and consequently the free radical elimination capacity.

Conclusion

The characterization data like %entrapment efficiency, %drug release, particle size, and zeta potential of optimized formulation was found to be equivalent to the predicted data (by BBD). *In vitro*, results show spherical morphology, compatibilities with ingredients, and intact structure of NAC in formulated SLNs. In addition to being much more effective than NAC alone, NACSLNs therapy also exhibited benefits that were equivalent to those of the well-known liverprotective and antioxidant compound SILY. Therefore, if they are to "see the light" of being therapeutically relevant, their biopharmaceutical betterment is a must. Although NAC's solubility and BA are important, it's rapid metabolism and subsequent elimination point to the necessity for packaging it into a sustained/prolonged release carrier system to increase its T1/2 and, in turn, mean resident time in the body, which will enable it to have an extensive physiological effect. According to the study, if NAC is placed into an appropriate delivery system like SLNs, it may be employed as a therapeutic agent to treat liver ailments.

Ethical approval

The Institutional Review Board of Nalanda College of Pharmacy authorized the animal research proposal (protocol code 318/Re/s/2001/CPCSEA, IAEC Approval No: NCOP/IAEC/00075).

Acknowledgements

The authors are thankful to the authority of KL College of Pharmacy, KL Deemed to be University, and Nalanda College of Pharmacy for providing the necessary facilities. The authors like to extend heartful thanks to the Late Prof. Uma Shankar Kulaidaivelu for having his intense faith and support in them.

References

Alam N, Bristi NJ, Rafiquzzaman (2013) Review on *in vivo* and *in vitro* methods evaluation of antioxidant activity. Saudi Pharmaceutical Journal 21(2): 143–152. https://doi.org/10.1016/j.jsps.2012.05.002

Assi RA, Abdulbaqi IM, Yee CS (2021) The evaluation of drug delivery nanocarrier development and pharmacological briefing for metabolic-associated fatty liver disease (Mafld): An update. Pharmaceuticals 14(3): e215. [MDPI AG] https://doi.org/10.3390/ph14030215

Atkuri KR, Mantovani JJ, Herzenberg LA, Herzenberg LA (2007) N-acetylcysteine-a safe antidote for cysteine/glutathione deficiency. Current Opinion in Pharmacology 7(4): 355–359. https://doi.org/10.1016/j.coph.2007.04.005

del Rio D, Stewart AJ, Pellegrini N (2005) A review of recent studies on malondialdehyde as toxic molecule and biological marker of oxidative stress. Nutrition, Metabolism and Cardiovascular Diseases [Elsevier] 15(4): 316–328. https://doi.org/10.1016/j.numecd.2005.05.003

El-Housiny S, Maii ASE, El-Attar YA, Salem HA, Attia D, Bendas ER, El-Nabarawi MA (2018) Fluconazole-loaded solid lipid nanoparticles topical gel for treatment of pityriasis versicolor: formulation and clinical study. Drug Delivery 25(1): 78–90. https://doi.org/10.1080/10717544.2017.1413444

Hsu YW, Tsai CF, Chuang WC, Wen KC, Ho YC, Lu FJ (2010) Protective effects of silica hydride against carbon tetrachloride-induced hepatotoxicity in mice. Food and Chemical Toxicology 48(6): 1644–1653. https://doi.org/10.1016/j.fct.2010.03.039

Khushboo S, Prabhu PP, Subramanyam EVS, Shabaraya R (2015) Development of new analytical methods and their validation for the determination of and n-acetylcysteine in bulk and marketed formulations.

Kim YS, Song MY, Park JD, Song KS, Ryu HR, Chung YH, Chang HK, Lee JH, Oh KH, Kelman BJ, Hwang IK, Yu IJ (2010) Subchronic oral toxicity of silver nanoparticles. Particle and Fibre Toxicology 7: 1–20. https://doi.org/10.1186/1743-8977-7-20

King EJ, Armstrong AR (1934) A convenient method for determining serum and bile phosphatase activity. Canadian Medical Association Journal 31: e376.

Madupoju B, Raju RS, Desu PK, Rao GSNK, Alavala RR, Amara RD, Chakravarthi G (2022) Development, characterization and optimization of N-acetylcysteine-loaded solid lipid particles: *In-vitro* and *in-vivo* study. International Journal of Drug Delivery Technology 12(3): 1129–1135. https://doi.org/10.25258/ijddt.12.3.34

Morisco F, Vitaglione P, Amoruso D, Russo B, Fogliano V, Caporaso N (2008) Foods and liver health. Molecular Aspects of Medicine 29(1–2): 144–150. https://doi.org/10.1016/j.mam.2007.09.003

Ohkawa H, Ohishi N, Yagi K (1979) Assay for lipid peroxides in animal tissues by thiobarbituric acid reaction. Analytical Biochemistry 95(2): 351–358. https://doi.org/10.1016/0003-2697(79)90738-3

Pandian KSR, Pavadai P, Vellaisamy S, Ravishankar V, Palanisamy P, Sundar LM, Chandramohan V, Sankaranarayanan M, Panneerselvam T, Kunjiappan S (2015) Formulation and evaluation of rutin-loaded solid lipid nanoparticles for the treatment of brain tumor. Naunyn-Schmiedeberg's Archives of Pharmacology volume 394: 735–749. https://doi.org/10.1007/s00210-020-02015-9

Pradhan SC, Girish C (2006) Hepatoprotective herbal drug, silymarin from experimental pharmacology to clinical medicine. Indian Journal of Medical Research 124(5): 49–504.

Rahal A, Kumar A, Singh V, Yadav B, Tiwari R, Chakraborty S, Dhama K (2014) Oxidative stress, prooxidants, and antioxidants: The interplay. BioMed Research International 2014: 1–19. https://doi.org/10.1155/2014/761264

Rahman MA, Ali A, Rahamathulla M, Salam S, Hani U, Wahab S, Warsi MH, Yusuf M, Ali A, Mittal V, Harwansh RK (2023) Fabrication of sustained release curcumin-loaded solid lipid nanoparticles (Cur-SLNs) as a potential drug delivery system for the treatment of lung cancer: Optimization of formulation and *in vitro* biological evaluation. Polymers 15(3): e542. https://doi.org/10.3390/polym15030542

Rampaka R, Ommi K, Chella N (2021) Role of solid lipid nanoparticles as drug delivery vehicles on the pharmacokinetic variability of Erlotinib HCl. Journal of Drug Delivery Science and Technology 66: e102886. https://doi.org/10.1016/j.jddst.2021.102886

Reitman S, Frankel S (1957) A colorimetric method for the determination of serum glutamic oxalacetic and glutamic pyruvic transaminases. American Journal of Clinical Pathology 160(5): aqad151. http://ajcp.oxfordjournals.org/

Ringoira S, Plumb J (1975) LDH isozymes of human t and b lymphocytes. Clinica Chimica Acta 60(3): 379–383. https://doi.org/10.1016/0009-8981(75)90081-9

Rotruck JT, Pope AL, Ganther HE, Swanson AB, Hafeman DG, Hoekstra WG (1973) Selenium: biochemical role as a component of glutathione peroxidase. Science 179(1973): 588–590. https://doi.org/10.1126/science.179.4073.588

Shrivastava S, Kaur CD (2020) Fabrication of mebendazole loaded solid lipid nanoparticles: Formulation, optimization, characterization, stabilization, and in-vitro evaluation. International Journal of Pharmaceutical Sciences and Drug Research 14(02): 262–268. https://doi.org/10.25004/IJPSDR.2022.140217

Thapa BR, Walia A (2007) Symposium: Newer diagnostic tests liver function tests and their interpretation. Indian Journal of Pediatrics 74: 663–671. https://doi.org/10.1007/s12098-007-0118-7

Upur H, Amat N, Blažeković B, Talip A (2009) Protective effect of *Cichorium glandulosum* root extract on carbon tetrachloride-induced and galactosamine-induced hepatotoxicity in mice. Food and Chemical Toxicology 47(8): 2022–2030. https://doi.org/10.1016/j.fct.2009.05.022

Weber D, Lutz W, Boll M, Stampfl A (2003) Hepatotoxicity and Mechanism of Action of Haloalkanes: Carbon Tetrachloride as a Toxicological Model. Critical Reviews in Toxicology 33(2): 105–136. https://doi.org/10.1080/713611034

Ye X, Feng Y, Tong Y, Ng KM, Tsao SW, Lau GKK, Sze C, Zhang Y, Tang J, Shen J, Kobayashi S (2009) Hepatoprotective effects of *Coptidis rhizoma* aqueous extract on carbon tetrachloride-induced acute liver hepatotoxicity in rats. Journal of Ethnopharmacology 124(1): 130–136. https://doi.org/10.1016/j.jep.2009.04.003